9.1 Materials

Lenalidomide (LND) was obtained as a gift sample from Apicore Pharmaceutical Ltd, Vadodara (India). Bovine serum albumin (BSA), acetic acid, gluteraldehyde and dialysis membrane (12000Da cut-off) were purchased from Himedia, Mumbai, India. Ethanol, hydrochloric acid, glacial acetic acid, phosphoric acid and Coomassie Brilliant Blue G-250 were purchased from Spectrochem Pvt Ltd, Mumbai (India). Lactoferrin was obtained as a gift sample from FrieslandCampina, Netherlands. Trehalose was purchased from SD Fine chemicals, Mumbai (India). HPLC grade acetonitrile and methanol were purchased from Renkem (India). Disodium hydrogen phosphate, potassium dihydrogen phosphate, sodium chloride, sodium acetate, sodium hydroxide, potassium sulphate, Tris-hydrochloride and dipotassium EDTA dihydrate were purchased from SD fine chemicals Pvt. Ltd., Mumbai, India. All other chemicals and solvents used were of analytical grade.

9.2 Equipments

- pH meter (Lab India Pvt. Ltd. India)
- Digital analytical balance (ATX224 Shimadzu, Japan)
- UV-Visible spectrophotometer (1800 Shimadzu, Japan)
- Cooling centrifuge (Remi equipment Pvt Ltd, India)
- Magnetic stirrer (Remi sci. Equipment, India)
- Deep freezer (EIE Inst. Ltd, Ahmedabad)
- Zetasizer (Nano ZS, Malvern ltd., UK)
- Differential Scanning Calorimeter (DSC-60-Shimadzu Corporation , Japan)
- Infrared Spectrophotometer (IR Affinity -1S,Shimadzu , Japan)
- Lyophilizer (Advantage 2.0 Bench Top Freeze Dryer/ Lyophilizer, SP Scientific, USA)

9.3 Methods

9.3.1 Preparation of lenalidomide loaded BSA nanoparticles (LNPs)

LND loaded albumin nanoparticles (LNPs) were prepared by desolvation method as reported earlier with slight modification (1). Briefly, BSA (16.67 mg/ml) was dissolved in double distilled water (pH was adjusted to 5.7 ± 0.2 using dilute acetic acid) under magnetic stirring. LND was added in the ethanol and sonicated in the bath sonicator for dissolvation of drug. For preparation of nanoparticles, LND containing ethanol (organic phase) was added drop wise in the aqueous phase at a constant flow rate of 1 ml/min under constant magnetic stirring (rpm = 700). Then gluteraldehyde (GA) (8 % w/v) was added for hardening of the prepared nanoparticles The nanoparticles were then separated by centrifugation at 16000 rpm for 30 min and washed three times with ethanol to remove excess GA. The prepared nanoparticles were freeze dried using trehalose (5% w/w) as cryoprotectant. Placebo albumin nanoparticles (PNPs) were prepared with the same method.

9.3.2 Optimization of LNPs by One Factor At a Time (OFAT) variable design

LNPs were optimized by OFAT design. Various process and formulation variables like drug concentration, polymer concentration, aqueous to organic ratio, cross-linker (gluteraldehyde) concentration, rate of addition of organic phase, effect of stirring speed, effect of pH, etc were screened and optimized for development of LNPs. As effect of BSA concentration was previously optimized for placebo nanoparticles (section 5.3.2.1), the optimized concentration of BSA (16.67 mg/ml) was used for preparation of LNPs. As LND is also contain amide functionality like TMZ, same aqueous phase (double distilled water having pH 5.7 ± 0.2) and pH was used as aqueous solvent.

9.3.2.1 Effect of aqueous to organic phase ratio

The effect of aqueous to organic phase ratio on quality attributes like particle size, PDI, % EE and % DL of LNPs were studied by varying the ratio from 1:1 to 1:3.

9.3.2.2 Effect of organic solvent

Based on the optimization results of TNPs, ethanol and acetone were selected for screening as organic phase and NPs were prepared. The effect of solvent was studied on the basis of particle size, PDI, % EE and % DL.

9.3.2.3 Effect of amount of gluteraldehyde

The effect of amount of GA (0.2 µl/mg of BSA - 0.98 µl/mg of BSA) on particle size, PDI, % EE and % DL of LNPs were studied. The amount of GA was varied from 10 µl to 40 µl for optimization.

9.3.2.4 Effect of rate of addition of organic phase

To study the effect of rate of addition of organic phase on the quality attributes like particle size, PDI and %EE, different batches were prepared by varying rate of addition from 0.25 ml/min to 1.5 ml/ min.

9.3.2.5 Effect of stirring speed

To study the effect of stirring speed of magnetic stirrer on the quality attributes like particle size, PDI and %EE, different batches were prepared by varying stirring speed 650-700 rpm and 950-1000 rpm.

9.3.2.6 Effect of drug concentration

Three different drug concentrations (based on the solubility of drug in ethanol) viz. 5 mg, 10 mg and 50 mg were used to prepare LNPs and its effect on particle size, PDI, % EE and % DL was observed to assess the effect

9.3.3 Surface modification of LNPs with lactoferrin (Lf) and it's optimization

Lactoferrin (Lf) was utilized for surface modification of LNPs and surface modification took place via electrostatic interaction between LNPs (negatively charged) and Lf (positively charged). Surface modification of LNPs with Lf was carried out using previously reported

method (2). Briefly, lyophilized LNPs were redispersed in Tris-EDTA buffer (pH 7.4) and kept on stirring at 500 rpm. Then equal volume of Lf solution (2 mg/ml in same buffer) was added drop wise in the LNPs dispersion under gentle stirring. Then the dispersion was kept on stirring for 1 h for adsorption of Lf over the LNPs. After 1 h, dispersion was centrifuged at 17000 rpm for 15 min at 4°C (2 cycles) to obtained surface modified LNPs (Lf-LNPs). The obtained Lf-LNPs were redispersed in water and lyophilized after adding trehalose (5% w/w) as cryoprotectant.

In the next step, Lf-LNPs were optimized by OFAT analysis on the basis of effect of Lf concentration (1 % w/v, 5 % w/v and 10 % w/v) and stirring time (1 h, and 3 h) on the particle size and zeta potential.

9.3.4. Lyophilization of LND loaded albumin nanoparticles (LNPs and Lf-LNPs)

The albumin nanoparticles (PNPs, LNPs and Lf-LNPs) aqueous dispersion with 5 % cryoprotectant (trehalose) was frozen in a refrigerator at –70°C for 12 hours. Then the samples were lyophilized using a lab freeze-dryer (Advantage 2.0 Bench Top Freeze Dryer/ Lyophilizer, SP Scientific, USA). The freeze-drying was conducted for 48 hours. After this, the vials were sealed with rubber caps (3).

9.3.5. Characterization of LND loaded albumin nanoparticles (LNPs and Lf-LNPs)

9.3.5.1 Particle size and PDI determination

The particle size and PDI of developed LNPs and Lf-LNPs were determined by Malvern Zetasizer as discussed in section 5.3.6.1. (1).

9.3.5.2 Zeta potential determination

The zeta potential of developed albumin nanoparticles LNPs and Lf-LNPs were measured by Malvern Zetasizer as mentioned in section 5.3.6.2. (1).

9.3.5.3 FTIR analysis

FTIR spectrum of developed LNPs and Lf-LNPs were measured with a FTIR spectrophotometer (IR Affinity -1S (Shimadzu, Japan) in range 400–4000 cm^{-1} using a resolution of 4 cm^{-1} (4).

9.3.5.4 XRD analysis

X-ray diffraction patterns of developed LNPs and Lf-LNPs were obtained using X-ray diffractometer (RigakuUltima IV; Japan) as mentioned in section 6.3.5.5. (4)

9.3.5.5 DSC analysis

DSC analysis of developed Lf-LNPs was carried out using a Differential Scanning Calorimeter (DSC-60, Shimadzu, Japan) by the method described in section 6.3.5.3 (4).

9.3.5.6 Morphology

Morphology of LNPs and Lf-LNPs were observed using transmission electron microscope (Philips CM200) (5).

9.3.6. Evaluation of LND loaded albumin nanoparticles (LNPs and Lf-LNPs)

9.3.6.1 Estimation of entrapment efficiency and drug loading

LND entrapment in the LNPs and Lf-LNPs was determined indirectly by measuring the amount of free LND in the supernatant using UV–visible spectrophotometer (Shimadzu UV-1700 at 330 nm (4). Then percentage entrapment efficiency (% EE) and drug loading (% DL) was determined using the formula:

$$\% EE = \frac{(\text{Total drug} - \text{Free drug})}{\text{Total drug}} \times 100 \text{.....Equation 9.1}$$

$$\% DL = \frac{\text{Entrapped drug}}{\text{Total weight of nanoparticles}} \times 100 \text{.....Equation 9.2}$$

9.3.6.2 *In-vitro* drug release

The *in-vitro* drug release studies were carried out using dialysis bag method at 37 °C under mild stirring (50 rpm) (6). Pure LND, LNPs and Lf-LNPs (equivalent to 5 mg drug) were taken into dialysis bags (MWCO = 12000), and were immersed into beakers containing 30 ml phosphate buffer saline (PBS, pH 7.4). At predetermined period, 1.0 ml of sample was withdrawn and same quantity of fresh buffer was added into the beaker to maintain sink condition. The amount of LND released was determined using spectrofluorophotometer (pl. refer section 3.8).

9.3.6.3 Modification efficiency of Lf on Lf-LNPs

The modification efficiency of Lf on Lf-LNPs was determined by previously reported method using Coomassie Brilliant Blue (Bradford protein estimation assay) (2). The un-adsorbed Lf molecules (free Lf) were estimated in the supernatant, after centrifuging the Lf-LNPs dispersion (17000 rpm, 30 min), by the method described in section 3.13.8 and % modification efficiency was determined by the below mentioned formula:

$$Modification\ efficiency\ (\%) = \left(\frac{Lf_{total} - Lf_{free}}{Lf_{total}}\right) \times 100 \text{.....Equation 9.3}$$

Where, Lf_{total} = Total amount of Lf added in the modification

Lf_{free} = Amount of un-adsorbed Lf

9.3.7 Bio-Interactions of Lf-LNPs

9.3.7.1 Interactions with plasma proteins

The interactions of Lf-LNPs with plasma protein were studied on the basis of method described in section 6.3.7.1 to assess the bio-stability of the prepared nanoparticles. Briefly, Lf-LNPs (5 mg/ml) were dispersed in PBS (pH 7.4) and mixed with protein solution (10% w/v) and incubated at 37°C in orbital shaker. After 4 h, the mixture was centrifuged at 12000 rpm and obtained pellet was redispersed in double distilled water. Then particle size and zeta potential of Lf-LNPs were measured (7,8).

9.3.7.2 Interactions with cell culture media (DMEM)

The interactions of Lf-LNPs with DMEM media were studied by dispersing Lf-LNPs (5 mg/ml) in PBS (pH 7.4) and mixed with DMEM media respectively and incubated at 37°C in orbital shaker. After 4 h, the mixture was centrifuged at 12000 rpm and obtained pellet was redispersed in double distilled water. Then particle size and zeta potential of nanoparticles dispersion LF-LNPs) were measured (7,9).

9.3.7.3 Interactions with serum

The interactions of Lf-LNPs with serum were studied by dispersing Lf-LNPs (5 mg/ml) in PBS (pH 7.4) and mixed with 50% v/v serum respectively and incubated at 37°C in orbital shaker. After 4 h, the mixture was centrifuged at 12000 rpm and obtained pellet was redispersed in double distilled water. Then particle size and zeta potential of nanoparticles dispersion (Lf-LNPs) were measured (8).

9.3.7.4 Haemolysis study

Haemolysis study of Lf-LNPs was performed on the basis of method described in section 6.3.7.4. Briefly, RBC solution (1 ml) was added to Lf-LNPs containing 1 mg equivalent amount of LND dispersed in 1ml of saline. For positive and negative control, 2.0% Triton-X100 (1ml) and 0.5% DMSO was used respectively. After treatment (with drug suspension, LNPs, Lf-LNPs, positive control and negative control), RBC dispersion was gently stirred to uniformly disperse RBCs. The treated dispersions were stored at 37°C for 30 min in incubator. After incubation, all the samples were centrifuged at 3000 rpm for 12 min at 4 °C to separate the RBC mass and the solutions were analyzed for UV absorbance at λmax of 540 nm against normal saline as a reference solution and percentage of haemolysis was determined (10,11).

9.3.8 Stability studies

The stability of the lyophilized LNPs and Lf-LNPs were investigated by storing samples at refrigerated condition (4°C) and at room temperature (25°C ±2°C) for 3 months. At regular time

interval of 1 month, samples were withdrawn and redispersed in saline solution to check particle size, assay and zeta potential (12,13) .

9.3.9 Statistical Data Analysis

Results are given as mean ± SD. Statistical significance was tested by two-tailed Student's t test or one-way ANOVA. Statistical significance was set at $P < 0.05$.

9.4 Results and discussion

9.4.1 Optimization of LNPs by OFAT design

LND loaded albumin nanoparticles (LNPs) were prepared by desolvation method. LNPs optimization was done on the basis of OFAT analysis. The aim was to optimize the process in such a way to obtain LNPs with minimum particle size and higher entrapment efficiency of LND along with to study the influence of process and formulation variables on quality attributes of LNPs like particle size, PDI, % EE and % DL.

9.4.1.1 Effect of aqueous to organic phase ratio

Various LNPs batches were prepared by varying the aqueous to organic phase ratio (1:1 to 1:3) and its effect on particle size, PDI, % EE and % DL was observed (Table 9.1 and figure 9.1). The results indicated that as the aqueous to organic phase ratio increased, particle size decreased while % EE and % DL increased. With 1:3 aqueous to organic phase ratio, smaller particle size (166.3 ± 1.5 nm) and lesser PDI (0.168 ± 0.011) was obtained with 90.90 % ± 1.3 % entrapment and 8.26 % ± 1.1 % drug loading of LND in BSA NPs. So this was selected as optimum aqueous to organic phase ratio. As discussed earlier, the formation of nanoparticles is dependent on the volume of organic solvent. If volume of organic phase is decreased, the amount of organic phase will not be sufficient for desolvation of the protein, and delayed precipitation and nucleation leading to formation of large aggregated particles with wide size distribution. On increasing the volume of organic solvent, smaller particles with narrow size distribution was obtained and after certain limit, further increase in volume of organic solvent did not affect size

but only affect size distribution. In case of EE, due to slow nucleation drug molecule got enough time to settle down in polymer matrix leading to increase in EE (5).

Table 9.1: Effect of aqueous to organic phase ratio on particle size, PDI, % EE and % DL of LNPs

Aqueous: organic phase ratio	Particle size (nm)	PDI	Entrapment efficiency (%)	Drug loading (%)
1:1	Particles not formed			
1:2	184.0 ± 1.9	0.239 ± 0.013	86.89 ± 1.50	7.80 ± 0.83
1:2.5	171.5 ± 2.5	0.122 ± 0.021	87.88 ± 2.90	7.99 ± 0.95
1:3	166.3 ± 2.9	0.168 ± 0.025	90.90 ± 1.30	8.04 ± 1.11

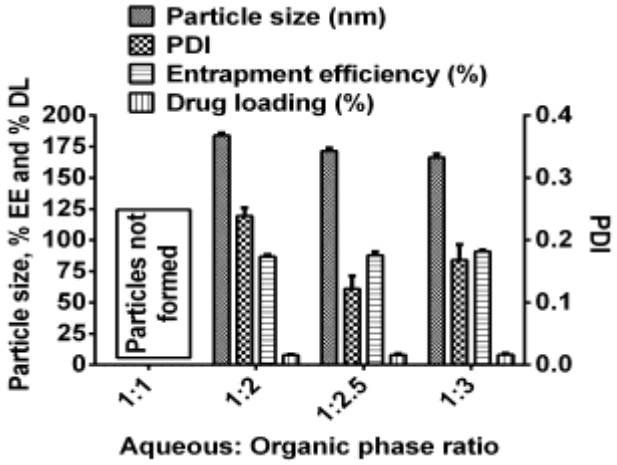

*** BSA – 16.67 mg/ml, Drug- 5.0 mg, GA- 20 µl , pH- 5.7± 0.2, rate of addition – 0.5 ml/min, stirring speed- 600-700 rpm**

Figure 9.1: Optimization of aqueous: organic phase ratio

9.4.1.2 Effect of organic solvent

Ethanol and acetone were selected as desolvating agent and their effect on particle size, PDI, % EE and % DL of LNPs were studied. The results (Table 9.2 and Figure 9.2) indicated that with acetone smaller particle size and more homogeneous dispersion of nanoparticles were formed but % EE and % DL decreased significantly. This may be due to degradation of LND in presence of acetone. In case of ethanol, although particle size and PDI were higher as compared to nanoparticles formed with acetone, % EE and % DL were also more. So on the basis of % EE and % DL, ethanol was selected as organic phase.

Table 9.2: Effect of organic solvent on particle size, PDI, % EE and % DL of LNPs

Organic solvent	Particle size (nm)	PDI	Entrapment efficiency (%)	Drug loading (%)
Ethanol	184.0 ± 1.5	0.239 ± 0.014	87.58 ± 2.30	8.04 ± 1.50
Acetone	140.0 ± 2.9	0.095 ± 0.021	40.40 ± 2.70	3.67 ± 2.80

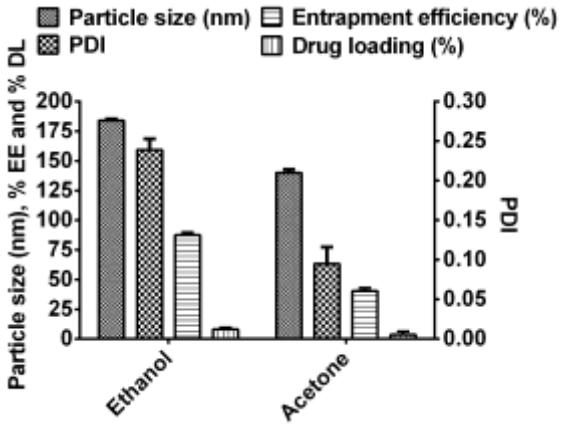

*** BSA – 16.67 mg/ml, Drug – 5.0 mg, GA- 20 µl, pH- 5.7± 0.2, aqueous: organic ratio – 1:2, rate of addition – 0.5 ml/min, stirring speed- 600-700 rpm**

Figure 9.2: Selection of organic solvent as desolvating agent

9.4.1.3 Effect of amount of gluteraldehyde

Different amount to gluteraldehyde (GA) was used to cross link the LNPs and results are summarized in Figure 9.3 and table 9.3. On the basis of obtained results, 20 µl of GA was found to be optimum as it showed highest EE (90.90 % ± 1.3 %) of LND in BSA NPs. Particle size, PDI and % DL was found to be 166.3 ± 1.5 nm, 0.168 ± 0.011 and 8.26 % ± 1.1 % respectively. The results indicated that no significant difference in particle size was observed up to 20 µl of GA and above this particle size increased. The obtained results may be correlated with the fact that in presence of higher amount of GA, the cross linking of nanoparticles becomes faster leading to inter particulate crosslinking causing aggregation and hence increase in particle size. The agglomeration formed sometimes displays porous natures through which drug leakage might take place leading to decrease in EE (1,5). Although no significant difference in % DL and % EE was observed. So, on the basis of higher % EE and %DL and lesser particle size, 20 µl of GA was selected as optimized amount.

Table 9.3: Effect of amount of gluteraldehyde on particle size, PDI, % EE and % DL of LNPs

Amount of GA	Particle size (nm)	PDI	Entrapment efficiency (%)	Drug loading (%)
10 µl	172.3 ± 2.5	0.236 ± 0.011	88.80 ± 1.50	8.07 ± 0.50
15 µl	164.8 ± 2.7	0.122 ± 0.015	88.58 ± 1.90	7.96 ± 0.97
20 µl	166.3 ± 3.1	0.168 ± 0.021	90.90 ± 2.30	8.26 ± 1.10
30 µl	194.2 ± 3.7	0.159 ± 0.029	87.81 ± 1.90	7.98 ± 0.83
40 µl	215.5 ± 3.5	0.251 ± 0.019	87.12 ± 1.67	7.99 ± 0.99

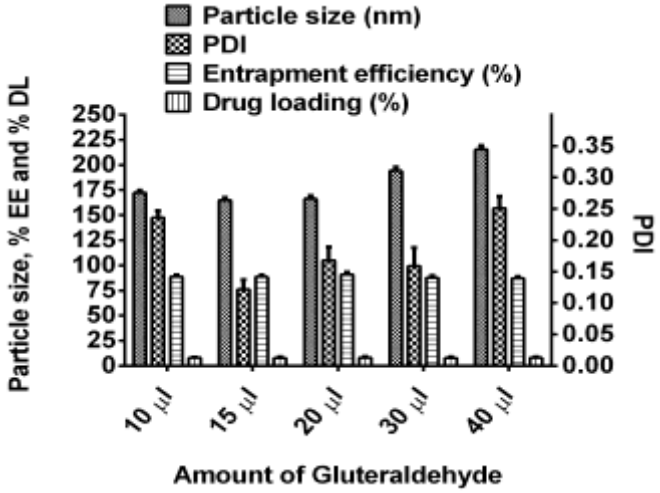

*** BSA – 16.67 mg/ml, Aq.: organic – 1:3, Drug- 5.0 mg, pH- 5.7± 0.2, rate of addition – 0.5 ml/min, stirring speed- 600-700 rpm**

Figure 9.3: Optimization of Gluteraldehyde amount

9.4.1.4 Effect of rate of addition of organic phase

Different LNPs batches were prepared by varying the rate of addition of organic phase and its effect on particle size, PDI, % EE and % DL was observed (figure 9.4 and table 9.4). The results indicated that after increasing the rate of addition of organic phase from 0.25 ml/min to 0.5 ml/min, initially particle size decreased and above 0.5 ml/min increase in particle size was observed. The increase in the particle size might be due to the fast desolvation process that leads to the larger aggregates and precipitation of albumin (17). In case of % EE and % DL, the results indicated no significant difference after increasing the rate of addition. The results obtained for % EE and % DL was accordance with reported literature (14). Based on the results, 0.5 ml/min was selected as optimized rate of addition.

Table 9.4: Effect of rate of addition of organic phase on particle size, PDI, % EE and % DL of LNPs

Rate of addition of organic phase (ml/min)	Particle size (nm)	PDI	Entrapment efficiency (%)	Drug loading (%)
0.25	228.2 ±1.9	0.276 ± 0.021	88.40 ± 1.90	8.01 ± 1.10
0.50	166.3 ± 2.5	0.168 ± 0.019	90.90 ± 1.50	8.26 ± 1.30
1.00	186.4 ± 2.9	0.209 ± 0.011	90.01 ± 1 .90	8.21 ± 1.90
1.50	197.8 ± 1.87	0.187 ± 0.017	90.58 ± 1.80	8.24 ± 1.51

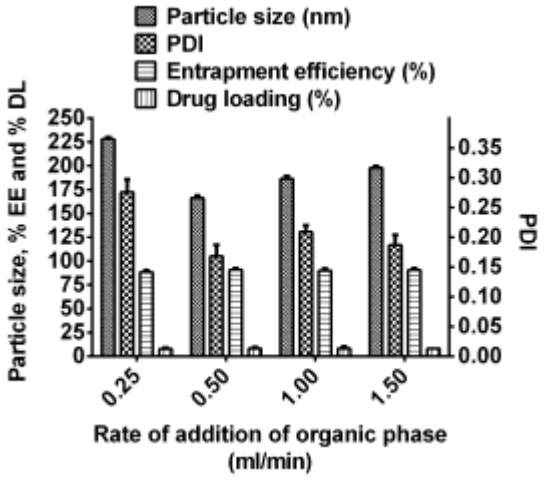

* BSA – 16.67 mg/ml, Aq.: organic – 1:3, Drug- 5.0 mg, pH- 5.7± 0.2, GA- 20 µl, stirring speed- 600-700 rpm

Figure 9.4: Optimization of rate of addition of organic phase

9.4.1.5 Effect of drug concentration

Various LNPs batches were prepared by varying the drug concentration (5 mg, 10 mg and 15 mg) and its effect on particle size, PDI, % entrapment efficiency and % drug loading was observed (figure 9.5 and table 9.5). The results indicated that with increasing the amount of drug (with respect to constant amount of polymer), particle size, % EE and % DL also increased.

When amount of drug increased from 10 mg to 15 mg, no significant change in the % EE was observed while % DL was increased. Although % DL was higher with 15 mg of drug, after sometime precipitation also occurred and batch was destabilized. So on the basis of the obtained results, 10 mg drug was selected as optimized concentration of drug. The obtained results may be correlated with the fact that with increasing the amount of drug, the amount of polymer is constant than amount of drug and the saturation of polymer takes place leading to less loading of drug inside polymer matrix (5,6).

Table 9.5: Effect of drug concentration on particle size, PDI, % EE and % DL of LNPs

Drug concentration (mg)	Particle size (nm)	PDI	Entrapment efficiency (%)	Drug loading (%)
5	166.3 ± 1.5	0.168 ± 0.013	84.00 ± 1.90	7.64 ± 2.50
10	170.9 ± 1.9	0.107 ± 0.015	92.00 ± 2.30	15.30 ± 1.50
15	181.6 ± 2.1	0.118 ± 0.011	91.50 ± 2.50	19.61 ± 1.10

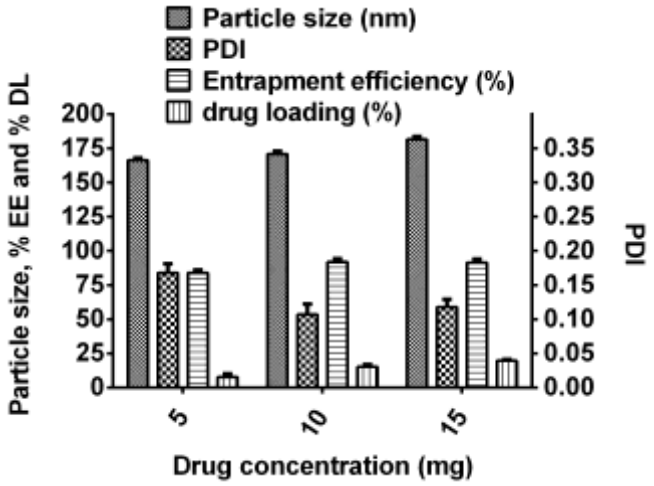

*** BSA – 16.67 mg/ml, Aq.: organic – 1:3, GA- 20 µl, pH- 5.7± 0.2, rate of addition – 0.5 ml/min, stirring speed- 600-700 rpm**

Figure 9.5: Optimization of drug concentration

9.4.1.6 Effect of stirring speed

The effect of speed on the quality attributes of LNPs were observed by varying the speed of magnetic stirring at two different speeds (650-700 rpm and 950-1000 rpm). The results indicated no significant effect on particle size, PDI, % EE and % DL of LNPs (figure 9.6 and table 9.6). So on the basis of results, lower rpm was selected as stirring speed for the preparation of LNPs.

Table 9.6: Effect of drug concentration on particle size, PDI, % EE and % DL of LNPs

Stirring speed (RPM)	Particle size (nm)	PDI	Entrapment efficiency (%)	Drug loading (%)
650-700	166.3 ± 2.5	0.168 ± 0.005	84.00 ± 2.50	7.64 ± 1.10
950-1000	169.1 ± 1.9	0.155 ± 0.007	86.56 ± 1.90	7.87 ± 1.30

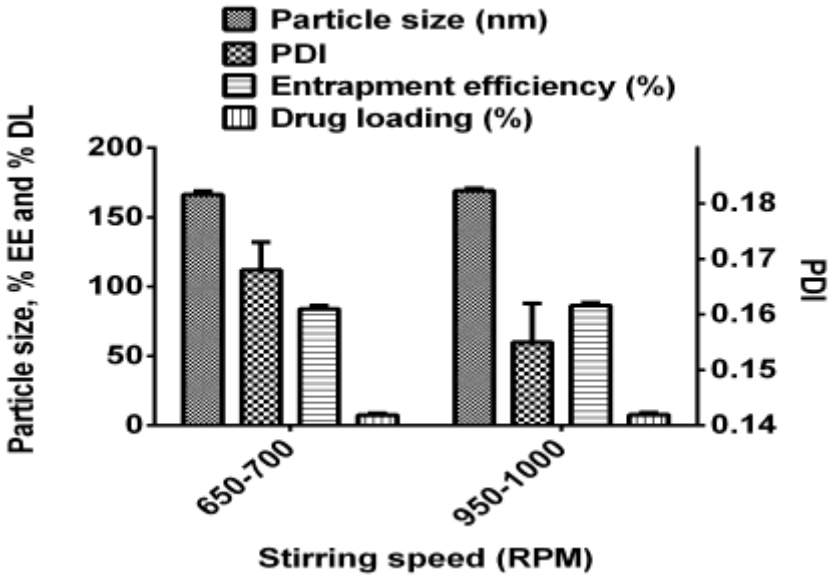

* **BSA – 16.67 mg/ml, Aq.: organic – 1:3, GA- 20 µl, pH- 5.7± 0.2, rate of addition – 0.5 ml/min, drug – 5.0 mg**

Figure 9.6: Optimization of stirring speed

The results of optimization are summarized in table 9.7

Table 9.7: Optimized values of different variables after OFAT analysis

Sr. No.	Name of variable	Range/ Constant value
1.	BSA Concentration	16.67 mg/ml
2.	Aqueous phase	Water (5.7±0.2 pH adjusted with dilute acetic acid)
3.	Organic phase	Ethanol
4.	Drug concentration	10 mg
5.	Aqueous. : Organic phase ratio	1:3
6.	Amount of GA	20 µl
7.	Rate of addition of organic phase	0.5 ml/min
8.	Stirring speed	650-700 RPM

9.4.2 Surface modification of LNPs with lactoferrin (Lf) and it's optimization

Surface modification of LNPs with Lf was done by means of electrostatic interaction between negative charge of LNPs and positive charge of Lf. As reported earlier, Lf contains positive charge and BSA contains negative charge on neutral pH so for the interaction between LNPs and Lf, pH 7.4 was selected and coating was optimized on the basis of particle size and zeta potential. For the optimization two variables (effect of time on coating of Lf over LNPs and effect of Lf concentration) were selected and optimization was done using OFAT analysis. For the optimization purpose, lyophilized LNPs (without cryoprotectant) were utilized which had initial particle size 200.6 ± 1.5 nm and zeta potential -16.7 ± 2.9 mV.

9.4.4.1 Effect of time of stirring on the coating of Lf over LNPs

For the optimization of time of coating of Lf over LNPs, 1 h and 3 h were selected as stirring time and its effect on particle size and zeta potential were studied. For the optimization, 1 % w/v Lf concentration and 1: 10 Lf to LNPs ratio was selected as constant variables. The results of optimization are shown in table 9.8. The results indicated time dependent increase in particle size

of Lf-LNPs. As time of stirring for coating increased, particle size of Lf-LNPs also increased which may be due to layering of Lf over the LNPs with the time (15). Stirring time did not show any significant effect on the zeta potential. Upon coating, the negative zeta potential of LNPs shifted towards neutral to positive side which indicated coating of positively charged Lf over the LNPs.

Table 9.8: Effect of time of stirring on the coating of Lf over LNPs

Sample	Stirring time (h)	Particle size (nm)	Zeta potential (mV)
LNPs	-	200.6 ± 1.5	- 16.7 ± 2.9
Lf (2 mg/ml)	-	-	+ 0.38 ± 0.7
Lf-LNPs	1	218.2 ± 2.7	+ 0.93 ± 0.5
Lf-LNPs	3	291.7 ± 3.5	+ 1.05 ± 0.9

9.4.4.2 Effect of Lf concentration

For the optimization of Lf concentration, three different concentrations 1 % w/v, 5 % w/v and 10 % w/v of Lf were selected and its effect on particle size and zeta potential were studied. For the optimization, 1 h stirring time and 1: 10 Lf to LNPs ratio was selected as constant variables. The results of optimization are shown in table 9.9. The results indicated concentration dependent increase in particle size of Lf-LNPs. As concentration of Lf increased, particle size of Lf-LNPs also increased which may be due to thick layer of Lf over the LNPs (15). At pH 7.4, the positive electrostatic surface potential of Lf produces a strong surface interaction, with the negative LPNs (zeta potential of -16.7 ± 2.9 mV) avoiding protein–protein interaction. This electrostatic interaction leads to formation of Lf monolayer coated onto the LPNs. Increase in Lf concentration did not show any significant effect on the zeta potential (16).

Table 9.9: Effect of Lf concentration

Sample	Lf concentration (% w/v)	Particle size (nm)	Zeta potential (mV)
LNPs	-	200.6 ± 1.5	- 16.7 ± 2.9
Lf alone	2 mg/ml	-	+ 0.38 ± 0.7
Lf-LNPs	1	218.2 ± 2.7	+ 0.93 ± 0.5
Lf-LNPs	5	1490.3 ± 3.5	+ 0.72 ± 0.3
Lf-LNPs	10	1655.7 ± 5.9	+ 0.28 ± 1.9

On the basis of obtained results, 1 % w/v of Lf concentration and 1 h stirring time was optimized for the preparation of Lf-LNPs.

9.4.2 Characterization of LND loaded albumin nanoparticles (LNPs and Lf-LNPs)

9.4.3.1 Particle size and PDI determination

Particle size and PDI of LNPs were found to be 128.4 ± 2.57 nm and 0.349 ± 0.005 respectively (figure 9.7) while in case of Lf-LNPs, particle size and PDI was found to be 148.1 ± 1.25 nm and 0.130 ± 0.011 respectively (figure 9.8). The enhancement in the size of Lf-LNPs was may be due to coating of Lf over LNPs which also confirmed the surface modification of LNPs with Lf.

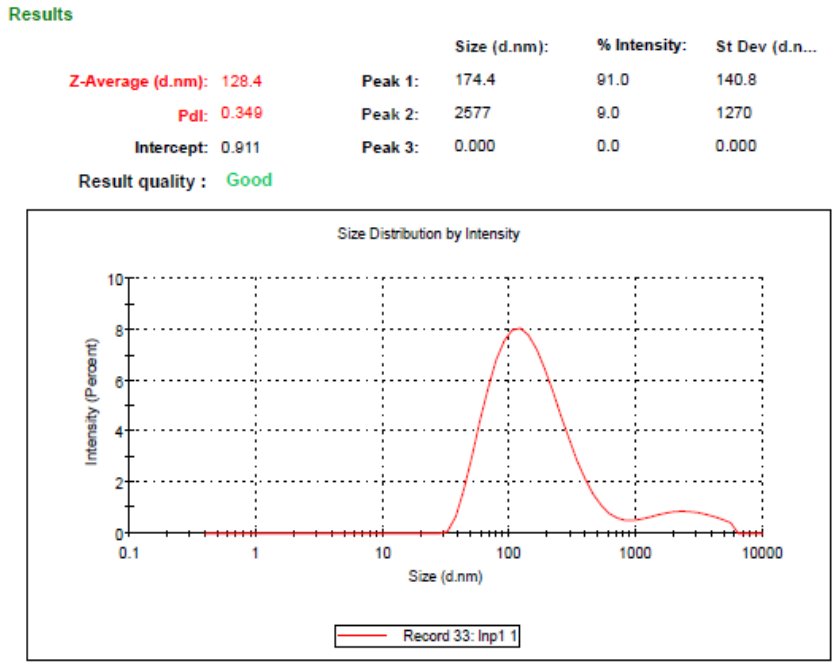

Figure 9.7 Particle size and PDI of optimized LNPs

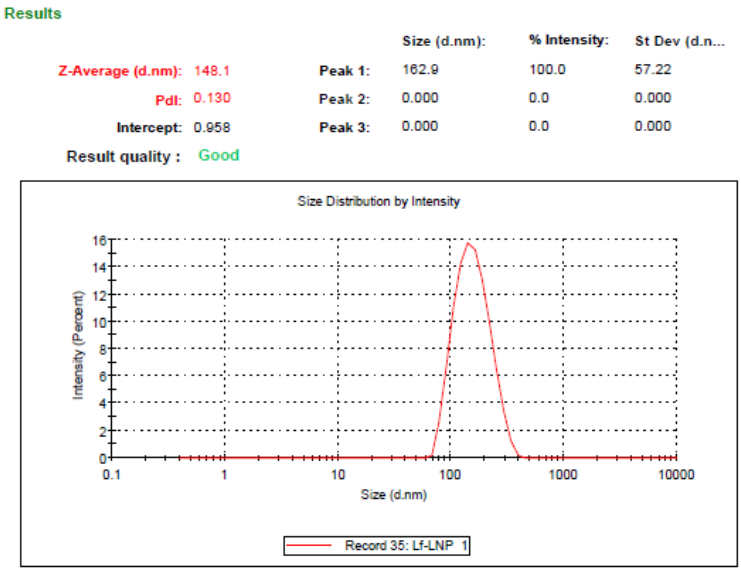

Figure 9.8 Particle size and PDI of optimized Lf-LNPs

9.4.3.2 Zeta potential determination

Zeta potential of LNPs was observed as -19.4 ± 1.9 mV (figure 9.9). As discussed earlier, above pH 4.3, BSA showed negative zeta potential thus LNPs also showed negative zeta potential. In case of Lf-LNPs, zeta potential was found to be + 0.96 ± 0.01 mV (figure 9.10). The results of Lf-LNPs indicated shifting of zeta potential towards positive size which may be due to coating of positively charged Lf (at pH 7.4 as charge on the Lf molecules are pH dependent) over the negatively charged LNPs. The zeta potential values also confirmed the surface modification of LNPs with Lf. The obtained results were also accordance with previously reported literature of Liu et al (17), in which they reported that after coating of Lf over the nano-liposomes the negative zeta potential of nano-liposomes shifted towards less negative / positive side.

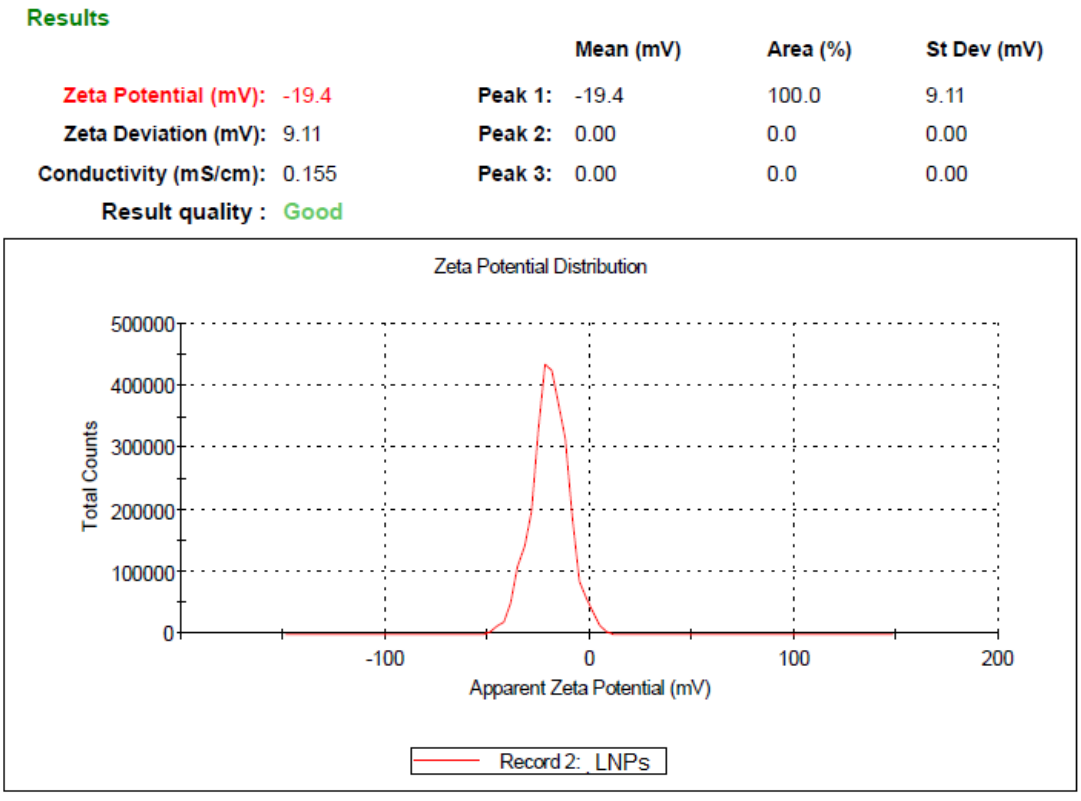

Figure 9.9: Zeta potential of optimized LNPs

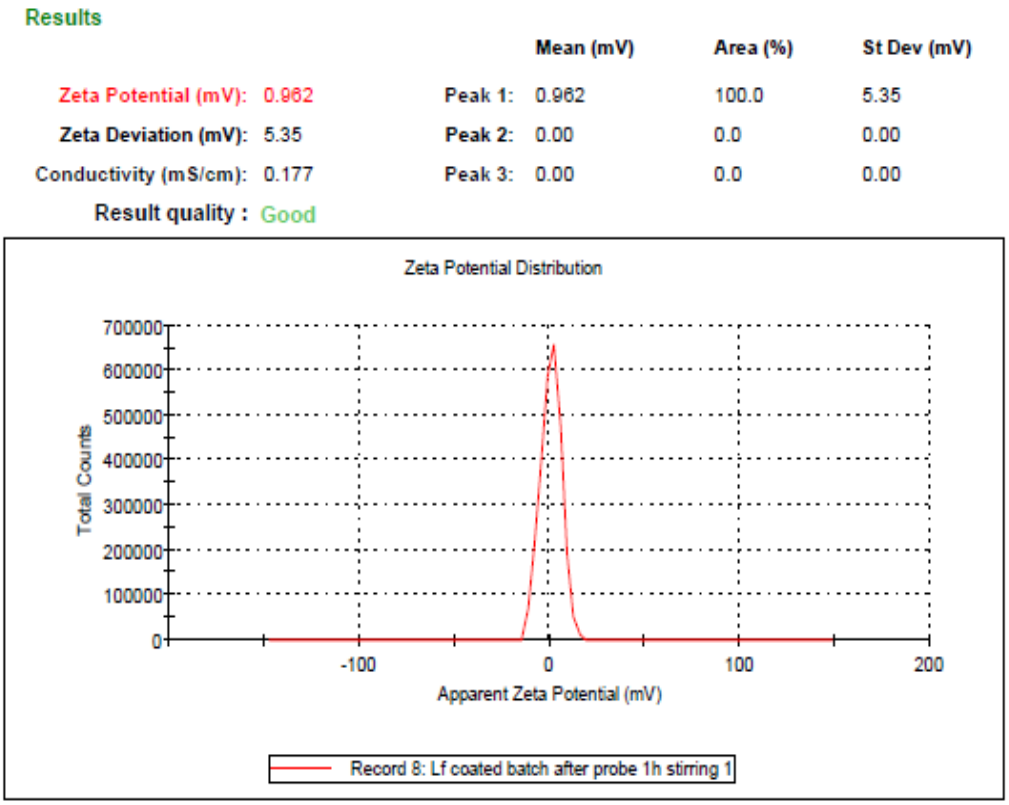

Figure 9.10: Zeta potential of optimized Lf-LNPs

9.4.3.3 FTIR analysis

The FTIR spectrum of BSA, LND, Lf, physical mixture, Lf-PNPs and Lf-LNPs are shown in figure 9.11 and all characteristic peaks are summarized in table 9.10. The FTIR spectrum of Lf-PNPs indicated that all characteristic peaks of BSA and Lf were present with lesser intensity as compare to pure BSA and Lf. In case of Lf-PNPs, all characteristic peaks of BSA, Lf and LND were present but the intensity of LND characteristic peaks were decreased which indicates that LND was present in Lf-LNPs (18,19)

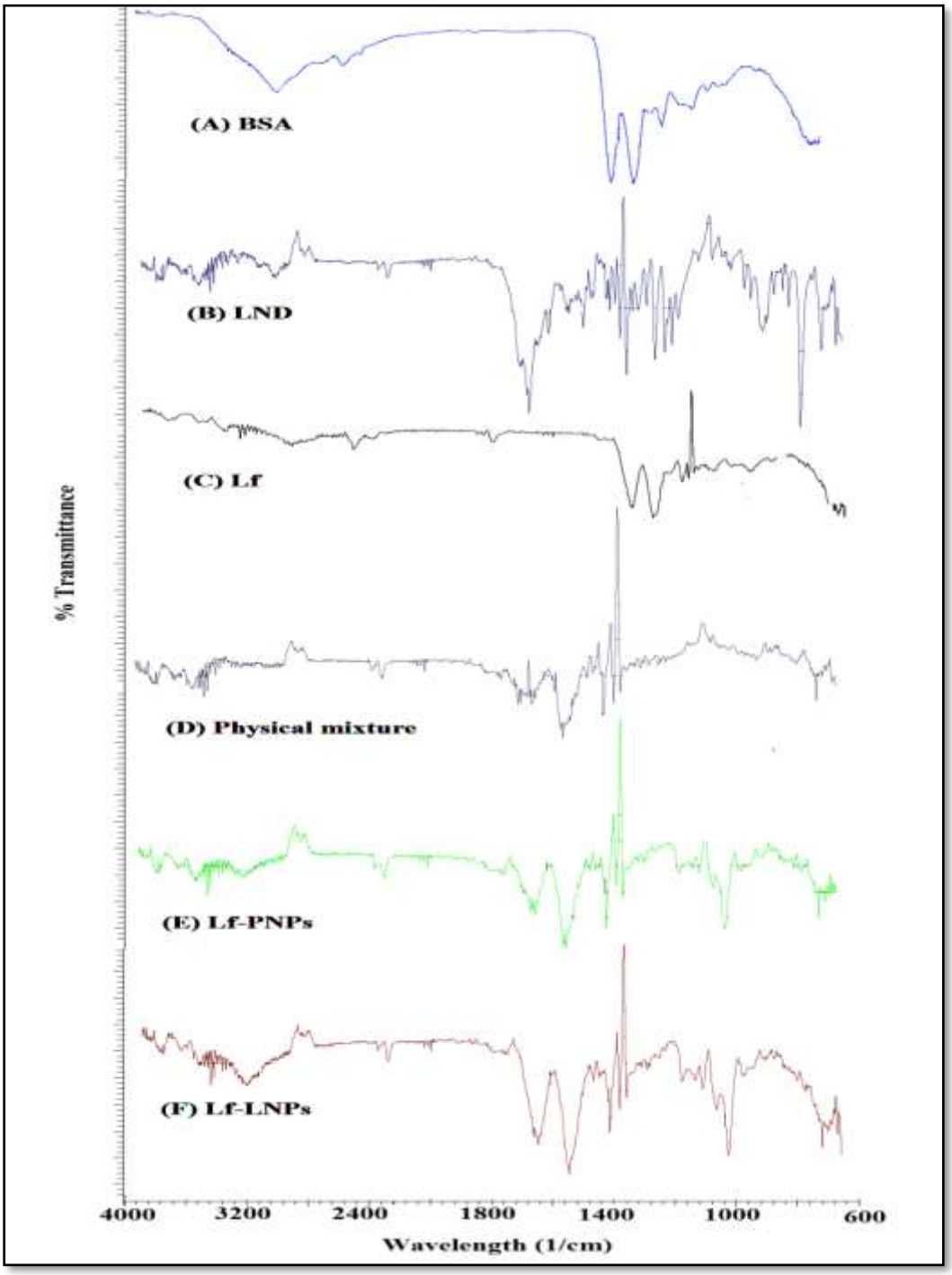

Figure 9.11: FTIR spectrum of BSA, LND, LF, physical mixture, Lf-PNPs and Lf-LNPs

Table 9.10: Summary of absorption peaks of FTIR spectrum of BSA, LND, LF, physical mixture, Lf-PNPs and Lf-LNPs

Functional moiety	Observed absorption peak (cm^{-1})	Functional group
LND	3408.22 cm^{-1}	–N-H stretch for amines
	3113.11 cm^{-1}, 3184.48 cm^{-1} and 3284.77 cm^{-1}	=C-H- (alkene) stretch
	1720.18 cm^{-1}	–C=O stretch contributed by aldehydes, ketones or amide group
	1670 cm^{-1}	-NH_2 stretching
BSA	3277.06	–NH stretching vibration
	2873 -2950	-C-H and -C-H methoxy stretching vibration
	1641.42	-C=O stretching vibrations of amide
	1535.34	-N–H bending -C–N stretching vibration of amide
Lf	1651 cm^{-1}	-C=O stretching vibrations of amide I
	1541 cm^{-1}	-N–H bending -C–N stretching vibration of amide
	3310 cm^{-1}	O-H stretching vibrations
	2850-3000 cm^{-1}	-C-H stretching vibration
	900-1200 cm^{-1}	-C-O, C-C stretch and –C-O-C and –C-O-H deformation of Lf
	700-600 cm^{-1}	-N-H wagging
Lf-PNPs	1791.87, 1639.49	-C=O stretching vibrations of amide
	1535.34	-N–H bending -C–N stretching vibration of amide
Lf-LNPs	1791.84 and 1641.42	-C=O stretching vibration of amide
	1534.34	-N–H bending -C–N stretching vibration of amide

9.4.3.4 DSC analysis

DSC thermograms of BSA, LND, Lf-PNPs and Lf-LNPs are shown in figure 9.12. As discussed earlier (section 5.4.4.3), the drug (LND) showed a sharp endothermic peak at 271.61^{o}C which indicates crystalline nature of LND. Thermogram of Lf-PNPs indicated amorphous nature of

developed NPs. Thermo gram of Lf-LNPs does not show any endothermic peak of LND which may be due to encapsulation of LND in the NPs in form of molecular dispersion (4).

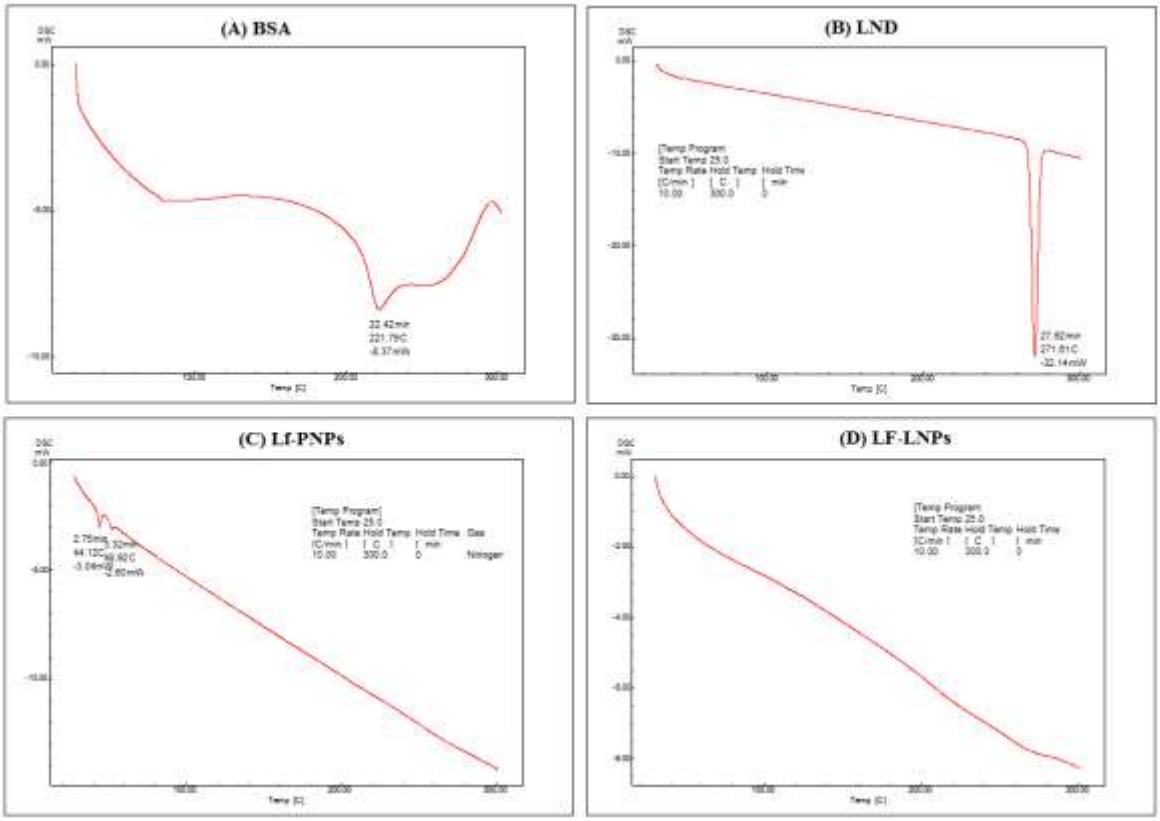

Figure 9.12: DSC thermograms of (A) BSA, (B) LND, (C) Lf-PNPs and (D) Lf-LNPs

9.4.3.5 XRD analysis

X-ray diffractograms (XRD) of pure LND, BSA, LNPs, Lf-PNPs and Lf-LNPs are shown in figure 9.13. LND showed characteristic sharp and intense peaks at 2θ values of 7.8°, 10.12°, 14.38°, 17.64°, 20.58°, 24.12° and 26.06° indicative of highly crystalline nature of drug (18). As mentioned earlier in section 6.4.3.5, XRD pattern of BSA did not show any sharp peaks representing their amorphous nature. The pattern of PNPs and Lf-PNPs indicated that the formed nanoparticles were amorphous. The XRD pattern of LNPs indicated amorphization of drug as sharp peaks of LND were not seen in the drug loaded nanoparticles. In case of Lf-LNPs, as compared to LNPs, some sharp peaks of LND were also observed with lesser intensity as

compared to pure drug which indicated that some amount of drug is also present in the periphery of the nanoparticles that may be due to surface modification of LNPs with Lf (18).

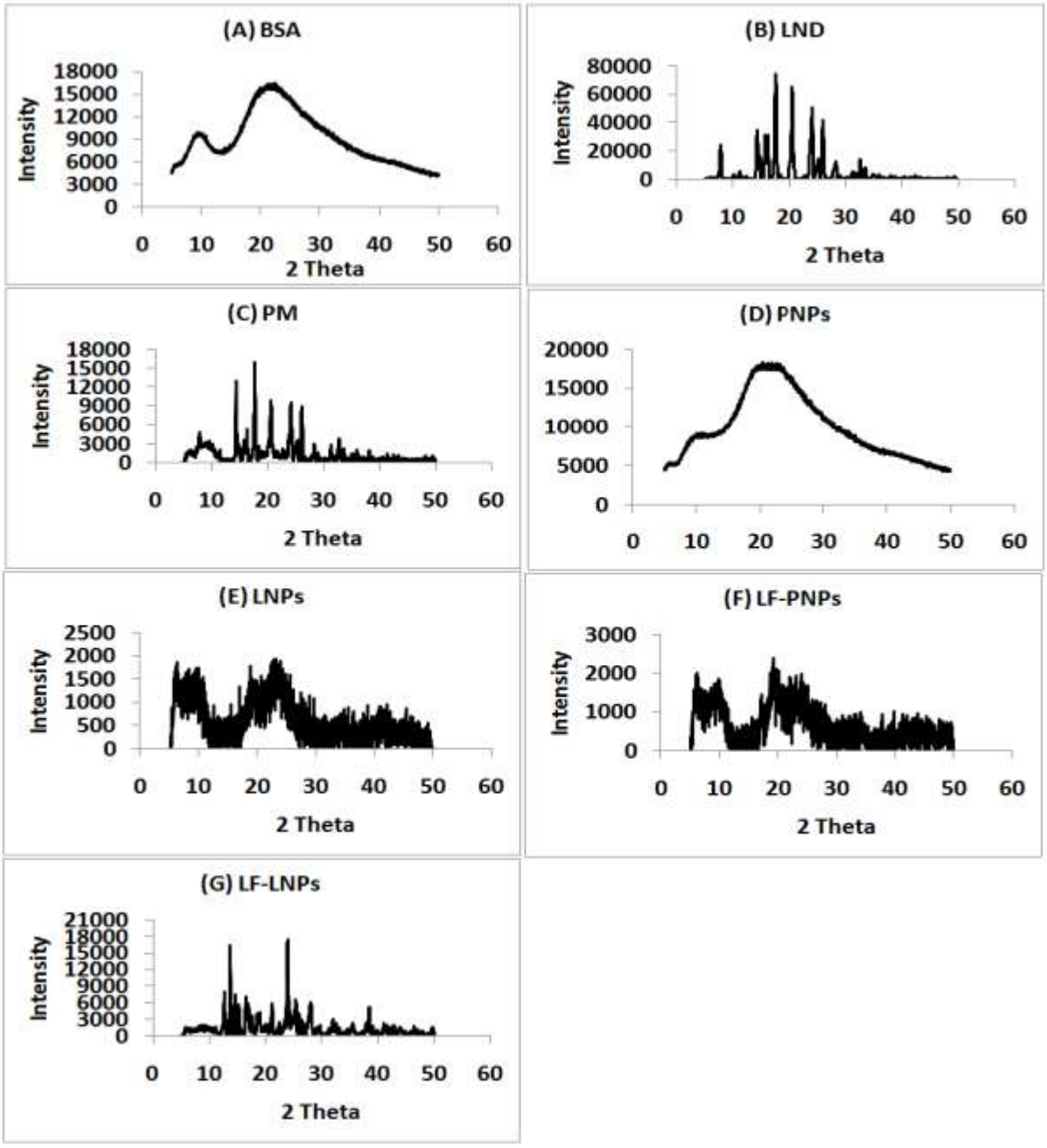

Figure 9.13: XRD diffractograms of (A) BSA, (B) LND, (C) Physical mixture (PM), (D) PNPs, (E) LNPs, (F) Lf-PNs and (G) Lf-LNPs

9.4.3.6 Morphology

Morphology of LNPs, and Lf-LNPs were determined by TEM analysis. TEM image of LNPs and Lf-LNPs showed spherical shape (figure 9.14 A and B respectively). TEM image of Lf-LNPs exhibited a dark core surrounded by a lighter gray rim likely corresponding to the Lf coating. Size of LNPs and Lf-LNPs obtained by TEM was lower than that obtained by zetasizer (DLS measurement). As mentioned earlier, higher particle size in case of DLS may be due to the presence of hydration layer while in case of TEM, size was measured in dried state [14].

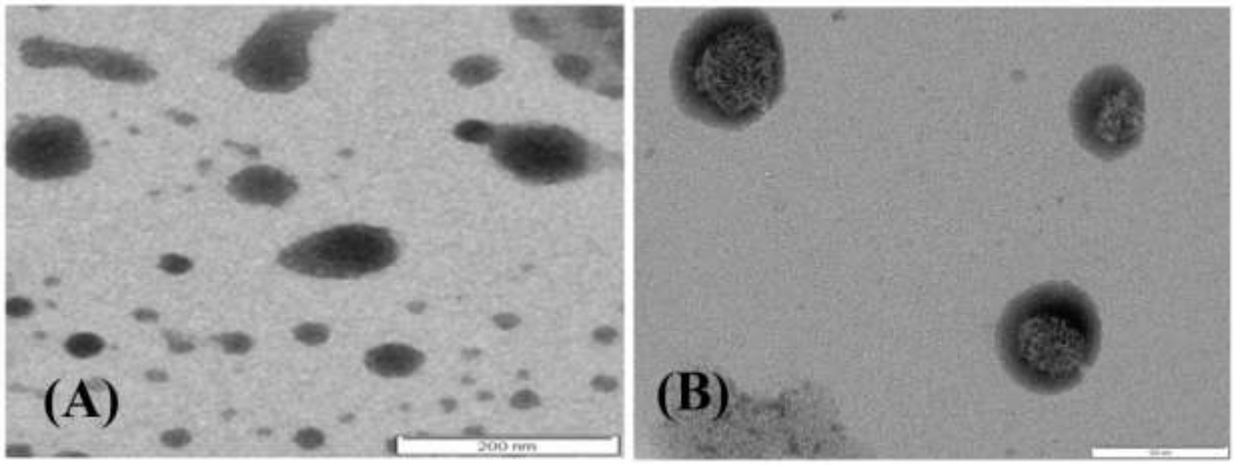

Figure 9.14 : TEM image of (A) LNPs and (B) Lf-LNPs

9.4.3 Evaluation of albumin nanoparticles (LNPs and Lf-LNPs)

9.4.4.1 Estimation of entrapment efficiency and drug loading

Percent entrapment efficiency of final optimized LNPs and Lf-LNPs were found to be 92.96 % ± 2.37 % and 90.05 % ± 2.87 % respectively while percent drug loading was found to be 12.13 % ± 1.77 % and 11.15 % ± 1.17 % respectively. As compared to LNPs, the decrease in the % EE of Lf-LNPs may be correlated with the fact that some amount of entrapped LND in LNPs may get released during coating of Lf with LNPs as the coating reaction took place in the aqueous condition for 1 hr. The decrease in the % DL can be correlated with the fact that in case of Lf-LNPs, total weight of the nanoparticles increased as compared to LNPs which led to reduction in the % DL because total weight of nanoparticles is inversely proportional to % DL.

9.4.4.2 *In-vitro* drug release

The results of cumulative *in-vitro* drug release (% CDR) from pure LND suspension, LNPs and Lf-LNPs dispersion are shown in table 9.11 and figure 9.15. Results of LND suspension indicated 87.84 % ± 1.9 % release of LND within 8 hr. In case of LNPs, biphasic drug release was observed in which 43.74 % ± 2.1 % drug was released within 4 hrs after that slow and sustained release of drug was observed up to 72 hrs (88.95 % ± 2.3 %). The initial fast release may be due to release of surface associated drug while slow and sustained release may be due to slow diffusion of drug from the LNPs. In case of Lf-LNPs, similar release pattern was obtained as observed for LNPs but initial drug release was observed up to 45 min (43.00 % ± 1.9 %) then slow and sustained release was observed up to 48 hr (84.26 % ± 2.3 %). As compared to LNPs, faster drug release was obtained from Lf-LNPs.

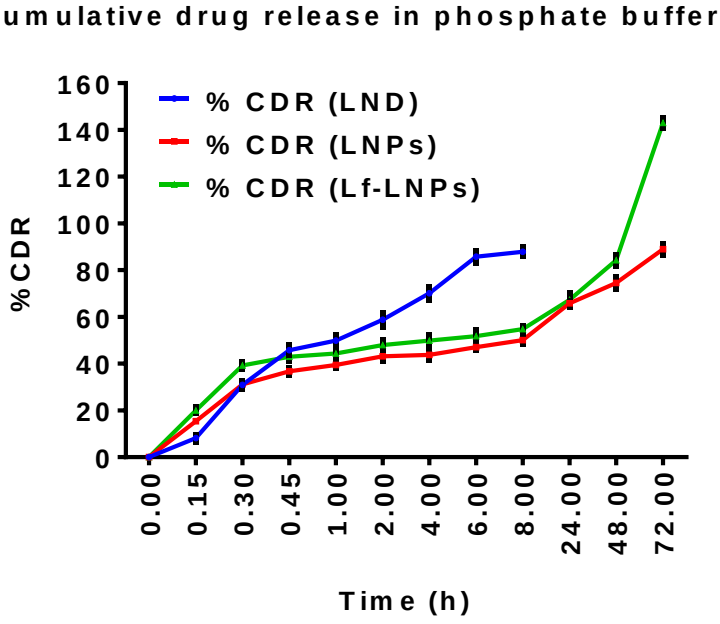

Figure 9.15: In vitro drug release study of LND, LNPs and Lf-LNPs in phosphate buffer pH 7.4

Table 9.11: *In-vitro* drug release in phosphate buffer pH 7.4

Time (h)	% CDR (LND)	% CDR (LNPs)	% CDR (Lf-LNPs)
0.00	0.00 ± 0.0	0.00 ± 0.0	0.00 ± 0.0
0.15	8.18 ± 1.5	15.39 ± 1.1	20.03 ± 1.3
0.30	30.91 ± 1.7	31.15 ± 1.3	39.20 ± 1.7
0.45	45.77 ± 2.1	36.76 ± 1.6	43.00 ± 1.9
1.00	49.91 ± 2.5	39.46 ± 1.4	44.39 ± 1.7
2.00	58.81 ± 2.9	43.18 ± 1.9	47.93 ± 2.1
4.00	70.15 ± 2.7	43.74 ± 2.1	49.84 ± 2.5
6.00	85.73 ± 2.5	47.03 ± 1.3	51.80 ± 2.7
8.00	87.84 ± 1.9	50.08 ± 1.5	54.80 ± 1.5
24.00		65.81 ± 1.2	67.29 ± 2.9
48.00		74.58 ± 2.5	84.26 ± 2.3
72.00		88.95 ± 2.3	143.05 ± 2.1

9.4.4.3 Modification efficiency of Lf on Lf-LNPs

The modification efficiency of Lf on Lf-LNPs was determined and results are summarized in table 9.12. The results indicated that increasing the amount of Lf, modification efficiency also increased but at the same time particle size also increased. For efficient targeting the particle size of nanoparticles should be preferably less than 200 nm. So keeping this in the mind lower concentration of Lf was finalized although it showed lower modification efficiency (31.78 % ± 2.3%) (2).

Table 9.12: Summary of modification efficiency of Lf on Lf-LNPs

Lf concentration (% w/v)	Particle size (nm)	Modification efficiency (%)
1	218.2 ± 2.7	31.78 ± 2.3
5	1490.3 ± 3.5	67.92 ± 1.9
10	1655.7 ± 5.9	81.86 ± 1.5

9.4.5 Bio-interaction studies of Lf-LNPs

The interaction of LND loaded albumin nanoparticles with plasma protein, cell culture media, serum proteins and RBCs were performed to evaluate the change in quality attributes (particle size and zeta potential) of LNPs and Lf-LNPs in existence of mentioned biological factors.

9.4.5.1 Interaction with plasma proteins

The interaction of Lf-LNPs with plasma protein was performed and results indicated no significant interaction between plasma proteins as no significant change in zeta potential and particle size was observed. Initial particle size and zeta potential of Lf-LNPs were 148.1 ± 3.25 nm and + 0.96 ± 0.5 mV respectively while after interaction with plasma proteins the obtained particle size and zeta potential were 150.3 ± 3.17 nm and + 0.91 ± 0.3 mV respectively. Hence it may be concluded that the developed Lf-LNPs were stable in presence of plasma proteins and can act as an efficient platform for targeting tumor without changing its quality attributes.

9.4.5.2 Interaction with cell culture medium

The interaction of Lf-LNPs with cell culture media (DMEM) was performed and results indicated no significant interaction between DMEM as no significant change in particle size and zeta potential was observed. Initial particle size and zeta potential of Lf-LNPs were 148.1 ± 3.25 nm and + 0.96 ± 0.5 mV respectively while after interaction with DMEM media obtained particle size and zeta potential were 149.1 ± 2.8 nm and + 0.93 ± 1.3 mV respectively. Hence it may be concluded that the developed Lf-LNPs were stable in cell culture media (DMEM).

9.4.5.3 Interaction with serum

The interaction of Lf-LNPs with serum was performed and results demonstrated no significant interaction between serum proteins as no significant change in particle size and zeta potential was observed. Initial particle size and zeta potential of HA-TNPs were 148.1 ± 3.25 nm and + 0.96 ± 0.5 mV respectively while after interaction with serum obtained particle size and zeta potential were 147 ± 2.71 nm and 0.89 ± 2.9 mV respectively. Hence it may be concluded that the developed Lf-LNPs were stable in serum.

9.4.5.4 Haemolysis studies

Haemolysis study was performed for developed Lf-LNPs. The absorbance values were obtained by scanning the samples by UV-Visible spectrophotometer and the percent haemolysis was calculated on the basis of equation 9.4. As mentioned earlier, the absorbance for positive control (Triton X- 100) and negative control (DMSO) was found to be 0.669 and 0.152 respectively. The % haemolysis for Lf-LNPs was found to be 0.58 % ± 0.25 %. The results demonstrated no significant haemolysis potential of developed Lf-LNPs as the % haemolysis for Lf-LNPs was found to be less than 2 (10) .

9.4.6 Stability studies

The results of stability studies (Table 9.13) indicated that prepared Lf-LNPs were stable at both refrigerated condition and room temperature (25°C) for three months as no significant change in particle size, assay and zeta potential was observed.

Table 9.13: Stability studies of lyophilized Lf-LNPs. Data is represented as mean ± SD (n=3)

Time (month)	Particle size (nm)	Zeta potential (mV)	% Assay
	Lf-LNPs	Lf-LNPs	Lf-LNPs
At refrigerated condition (4 °C)			
0	148.1 ± 1.25	0.96 ± 0.01	100 % ± 1.51%
1	147.7 ± 2.31	0.95 ± 0.01	99.7 % ± 3.09%
2	146.5 ± 3.17	0.95 ± 0.02	98.9 % ± 3.81%
3	146.1 ± 4.39	0.93 ± 0.03	98.1 % ± 4.13%
At room temperature (25°C ±2°C and 65% ± 5% relative humidity)			
0	148.1 ± 1.25	0.96 ± 0.01	100 % ± 1.51%
1	147.9 ± 2.69	0.95 ± 0.01	99.7 % ± 3.73%
2	147.1 ± 4.03	0.94 ± 0.03	99.2 % ± 4.01%
3	146.5 ± 4.97	0.93 ± 0.04	98.6 % ± 4.93%

References

1. Kamali M, Dinarvand R, Maleki H, Arzani H, Mahdaviani P, Nekounam H, et al. Preparation of imatinib base loaded human serum albumin for application in the treatment of glioblastoma. RSC Adv. 2015 Jul 16;5(76):62214–9.

2. Xu Y, Asghar S, Yang L, Li H, Wang Z, Ping Q, et al. Lactoferrin-coated polysaccharide nanoparticles based on chitosan hydrochloride/hyaluronic acid/PEG for treating brain glioma. Carbohydr Polym. 2017 Feb 10;157:419–28.

3. Anhorn MG, Mahler H-C, Langer K. Freeze drying of human serum albumin (HSA) nanoparticles with different excipients. Int J Pharm. 2008 Nov;363(1–2):162–9.

4. Jain D, Bajaj A, Athawale R, Shrikhande S, Goel PN, Nikam Y, et al. Surface-coated PLA nanoparticles loaded with temozolomide for improved brain deposition and potential treatment of gliomas: development, characterization and in vivo studies. Drug Deliv. 2016;23(3):999–1016.

5. Huang D, Chen Y-S, Rupenthal ID. Hyaluronic Acid Coated Albumin Nanoparticles for Targeted Peptide Delivery to the Retina. Mol Pharm. 2017 06;14(2):533–45.

6. Fang C, Wang K, Stephen ZR, Mu Q, Kievit FM, Chiu DT, et al. Temozolomide nanoparticles for targeted glioblastoma therapy. ACS Appl Mater Interfaces. 2015 Apr 1;7(12):6674–82.

7. Song Z, Lu Y, Zhang X, Wang H, Han J, Dong C. Novel curcumin-loaded human serum albumin nanoparticles surface functionalized with folate: characterization and in vitro/vivo evaluation. Drug Des Devel Ther. 2016;10:2643–9.

8. Katas H, Hussain Z, Awang SA. Bovine Serum Albumin-Loaded Chitosan/Dextran Nanoparticles: Preparation and Evaluation of Ex Vivo Colloidal Stability in Serum [Internet]. Vol. 2013, Journal of Nanomaterials. Hindawi; 2013 [cited 2020 Oct 6]. p. e536291. Available from: https://www.hindawi.com/journals/jnm/2013/536291/

9. Pandey A, Singh K, Patel S, Singh R, Patel K, Sawant K. Hyaluronic acid tethered pH-responsive alloy-drug nanoconjugates for multimodal therapy of glioblastoma: An intranasal route approach. Mater Sci Eng C Mater Biol Appl. 2019 May;98:419–36.

10. Zhang G-S, Hu P-Y, Li D-X, He M-Z, Rao X-Y, Luo X-J, et al. Formulations, Hemolytic and Pharmacokinetic Studies on Saikosaponin a and Saikosaponin d Compound Liposomes. Molecules. 2015 Apr;20(4):5889–907.

11. Yadav AK, Agarwal A, Rai G, Mishra P, Jain S, Mishra AK, et al. Development and characterization of hyaluronic acid decorated PLGA nanoparticles for delivery of 5-fluorouracil. Drug Deliv. 2010 Nov;17(8):561–72.

12. Bharti N, Harikumar SL, Buddiraja A. Development and characterization of albumin nanoparticles for pulmonary drug delivery. :7.

13. Chitkara D, Kumar N. BSA-PLGA-based core-shell nanoparticles as carrier system for water-soluble drugs. Pharm Res. 2013 Sep;30(9):2396–409.

14. Nouri A, Rafati H. Preparation and Characterization of Paclitaxel-Loaded Human Serum Albumin (HSA) Nanoparticles Using Desolvation Technique; Effect of Manufacturing Parameters on Particle Characteristics [Internet]. American Scientific Publishers; 2017 [cited 2020 Apr 27]. Available from: https://www.ingentaconnect.com/content/asp/jobn/2017/00000011/00000004/art00004

15. Abdelmoneem MA, Mahmoud M, Zaky A, Helmy MW, Sallam M, Fang J-Y, et al. Decorating protein nanospheres with lactoferrin enhances oral COX-2 inhibitor/herbal therapy of hepatocellular carcinoma. Nanomed. 2018 Oct 1;13(19):2377–95.

16. Fulgione A, Nocerino N, Iannaccone M, Roperto S, Capuano F, Roveri N, et al. Lactoferrin Adsorbed onto Biomimetic Hydroxyapatite Nanocrystals Controlling - In Vivo - the Helicobacter pylori Infection. Santos HA, editor. PLOS ONE. 2016 Jul 6;11(7):e0158646.

17. Liu W, Kong Y, Tu P, Lu J, Liu C, Liu W, et al. Physical–chemical stability and in vitro digestibility of hybrid nanoparticles based on the layer-by-layer assembly of lactoferrin and BSA on liposomes. Food Funct. 2017;8(4):1688–97.

18. Karri VVSR, Dhandapani NV, Mannemala SS, Radhakrishna K, Mulukutla S, Sudunagunta D. Ameliorating the antitumor activity of lenalidomide using PLGA nanoparticles for the treatment of multiple myeloma. Braz J Pharm Sci [Internet]. 2017 [cited 2020 Oct 21];53(2). Available from: http://www.scielo.br/scielo.php?script=sci_arttext&pid=S1984-82502017000200602&lng=en&tlng=en

19. Martins JT, Santos SF, Bourbon AI, Pinheiro AC, González-Fernández Á, Pastrana LM, et al. Lactoferrin-based nanoparticles as a vehicle for iron in food applications - Development and release profile. Food Res Int Ott Ont. 2016 Dec;90:16–24.